Journal of Thermal Analysis and Calorimetry, Vol. 76 (2004) 975–983

PHASE DIAGRAM INVESTIGATION AND THERMODYNAMIC STUDY OF Os–B SYSTEM

L. Stuparević and D. Živković[*]

University of Belgrade, Technical Faculty, Department of Metallurgy, VJ 12, 19210 Bor, Serbia and Montenegro

(Received September 19, 2003; in revised form January 5, 2004)

Abstract

The constitution of the Os–B system was investigated in this work. The phase regions were determined by metallographic investigations. The existence of the following borides was confirmed: $OsB_{1.1}$ (*hex.*), Os_2B_3 (*hex.*) and OsB_2 (*orthorh.*), while the new high temperature Os_2B_3 compound with a not yet identified structure was observed. $OsB_{1.1}$ melts congruently at 1820±15°C and OsB_2 at 1870±15°C, while the solid solubility of B in Os was found to be less than 0.5 at%B. Considering thermodynamic study of this system, the activities and activity coefficients for osmium and boron were determined in temperature interval 3300–3500 K, based on the known liquidus and solidus lines from phase diagram, according to calculation procedure given by Rao and Belton.

Keywords: alloy thermodynamics, Os–B system, phase diagram

Introduction

Several investigations on Os–B system, considering the phase diagram construction and phase equilibria determination, have been reported in literature by Arronson *et al*. [1, 2], Lundstram [3], Jantsch *et al.* [4] and Hassler [5]. Further, there are phase equilibria data on different Os–B based multicomponent systems, such as La–Os–B, Pr–Os–B system [6], Pu–Os–B system [7] and Ce–Os–B system [8]. Some of the references are dealing with the researches of superconductivity behaviour, which is characteristic for Os–B system and Os–B based systems [4, 9, 10]. Such materials are considered as plasma sprayable, also.

Concerning the thermodynamic data for this binary system, there are no adequate references in literature, except the work of Niessen [11], who determined the heats of formation for different osmium borides. The main reason for such a data lack is the high investigating temperature, which causes many difficulties in the experimental procedure.

In order to give a further contribution to more complete knowledge of the Os–B system, the phase diagram was established in this work by means of metallographical

* Author for correspondence: E-mail: jmm@eunet.yu or dzivkovic@tf.bor.ac.yu

1388–6150/2004/ $ 20.00

Akadémiai Kiadó, Budapest
Kluwer Academic Publishers, Dordrecht

analysis. The structure and composition of three previously reported [1–3] osmium borides $OsB_{1.1}$ (*hex*.), Os_2B_3 (*hex*.) and OsB_2 (*orthorh*.) were affirmed, and additionally a high temperature modification of Os_2B_3 (*hex*.) with a different *c*/*a* ratio was found. Thermodynamic analysis done according to Rao–Belton calculation procedure [12], which is based on the known liquidus and solidus lines of the phase diagram, is also presented in this paper.

Experimental procedure

Powder mixtures of high purity (>99.5%) osmium and boron were pressed into pellets (mass of 2 g) and than arc-melted under purified argon atmosphere (99.9999%) in a water-cooled crucible. To assure a sufficient homogeneity, samples were cut and remelted for several times. The samples were drop shaped.

Heat treatment and melting-point measurements were carried out in a tungsten mesh resistance furnace by using hot pressed boron nitride crucibles at several temperatures between 1300 and 2000 K.

The liquidus and liquidus-solidus lines were measured by pyrometrical melting-point measurements using two-color pyrometer. This method enables the observation of all changes on the sample surface during the melting and solidification processes.

Considering that the investigated alloys are very hard and chemically resistant, a lot of knowledge and experience were needed to prepare correctly the samples for metallographical investigations. The samples with higher boron content, and specially where boron appears as a separate phase, were brittle. During the mechanical preparation the boride phase shows tendency of throwing up from the surface. Metallography was used for the determination of phases and their regions and structural analysis was done by optical microscopy. The samples were ground on silicon water resistance paper (220, 500, 800, 1200, 4000) and polished on silk with 1 μm diamond paste. As for the appropriate etchant, fine results could be achieved by revealing of osmium borides with $H_2O+H_2O_2+HF$ (4:1:1).

Theoretical consideration

Thermodynamic investigations in this paper was done analytically using the Rao–Belton calculation procedure [12]. The main theoretical considerations of the method used will be given.

In some binary systems it is possible to calculate the activity coefficients of components in liquid solutions from the locations of the liquidus and solidus lines on the phase diagrams. For systems of simple eutectic type, with little or no terminal solid solubility, this method offers a mean of obtaining activity coefficients of acceptable accuracy.

In the case of an *a*–*b* eutectic system with small terminal solid solubility of Me (*b*) in Me (*a*) the following equilibrium reaction could be written:

$$\text{Me}\,(a) - \text{Me}\,(b)\ (\text{liquid alloy}) = \text{Me}\,(b)\ (\text{pure, solid})\ \text{at}\ T \qquad (1)$$

which means that activity of Me (*a*)-component is less than 1. Further, this can be expressed as

$$G_{\mathrm{Me(a)}} = G^{0}_{\mathrm{(a)(l)}} + RT\ln a_{\mathrm{(a)\ (l)}} = G_{\mathrm{(a)\ (s)}} = G^{0}_{\mathrm{(a)(s)}} + RT\ln a_{\mathrm{(a)\ (s)}} \quad (2)$$

where $a_{\mathrm{Me(a)\ (l)}}$ and $a_{\mathrm{Me(a)\ (s)}}$ are activities of Me (*a*)-component in liquid (related to pure liquid Me (*a*) in the standard state) and solid phase (related to pure solid Me (*a*) in the standard state), respectively. When solubility of Me (*b*) in the Me (*a*) is not too high, it can be assumed that solid phase is amenable to Raoult law, so $a_{\mathrm{Me(a)\ (s)}} = x^{\mathrm{s}}_{\mathrm{Me(a)}}$. Rearranging Eq. (2) one can obtain

$$\log a_{\mathrm{Me(a)\ (l)}} = \log x^{\mathrm{s}}_{\mathrm{Me(a)}} - \Delta G^{0}_{\mathrm{s}\rightarrow \mathrm{l[Me(a)]}}/2.303RT \quad (3)$$

which is the basic equation for the calculation of $a_{\mathrm{Me(a)(l)}}$ at different liquidus temperatures *T*.

When values for activities of Me (*b*) – component in liquid alloys of different compositions at the liquidus temperature are calculated, the activity coefficients at the investigated temperature *T'* could be calculated assuming regular solution behavior for the melts as follows [12]

$$\gamma' = \gamma_{\mathrm{i}}^{(\mathrm{T/T'})} \quad (4)$$

For the systems, where no data are available or where are difficulties in experimental research, this method could be very useful in the thermodynamic analysis and obtaining the activity-composition relation for the investigated composition range.

Results and discussion

Phase diagram investigation was done by metallographic analysis of more than a hundred samples investigated in order to identify present phases in this system. All borides were determined by metallographic technique, only it was not possible to see the difference between the low and high temperature Os_2B_3 phases. Some microstructure details, obtained by optical microscopy for the investigated samples, are presented in Figs 1–6.

As it is shown, it was difficult to homogenize the arc-melted samples, which were annealed at 1350, 1550, 1630 and 1740°C for 10 to 48 h, depending on a constitution. The microscopic analysis data gave the information about the number, amount and shape of present phases, which enable further constitution of the phase diagram, as shown in Fig. 7. More samples were investigated in the middle of the concentration region, because it was more difficult for analysis. After long time of homogenization at different temperatures, it was easy to identify single- or two-phase regions. Only for $Os_{60}B_{40}$ sample, which looks like a single phase at different temperatures, the results obtained by X-ray technique showed the presence of two phases [4] – the high temperature Os_2B_3 (*hex*.) phase and low temperature Os_2B_{3+x} (*hex*.) phase with a smaller *c/a* ratio, which could be constituted peritectically. As it needed a very long homogenization time for

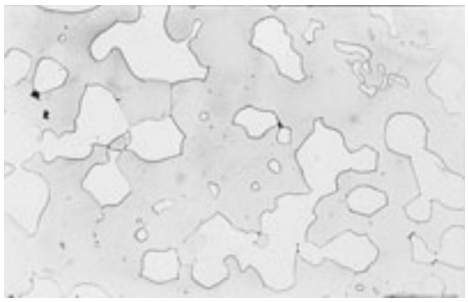

Fig. 1 $Os_{58}B_{42}$, arc melted and annealed at 1550°C, 10 h; Os (light)+$OsB_{1.1}$, etched; ×500

Fig. 2 $Os_{40}B_{60}$, arc melted and annealed at 1550°C, 10 h; Os_2B_3 (dark)+OsB_2 (light), etched; ×500

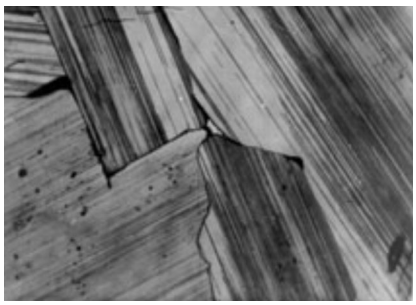

Fig. 3 $Os_{38}B_{62}$, arc melted and annealed at 1630°C, 48 h; Os_2B_3 phase; ×200

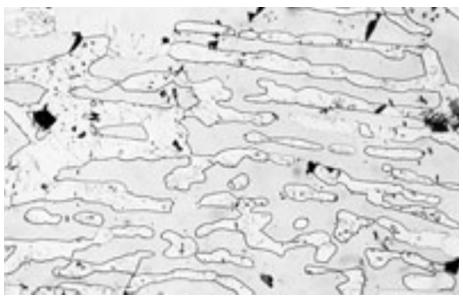

Fig. 4 $Os_{35}B_{65}$, arc melted and annealed at 1550°C, 10 h; Os_2B_3 (dark)+OsB_2 (light), etched; ×500

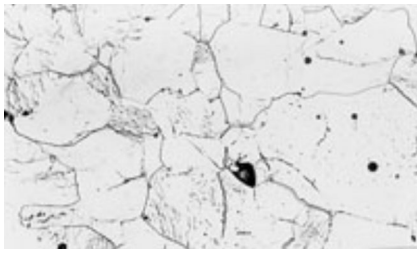

Fig. 5 $Os_{31}B_{69}$, arc melted and annealed at 1550°C, 10 h; OsB_2 single phase, etched; ×500

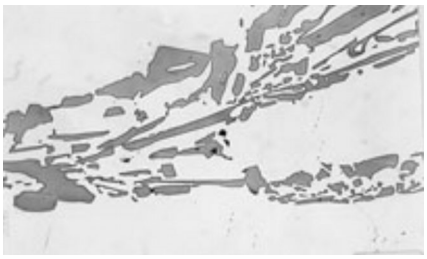

Fig. 6 $Os_{25}B_{75}$, arc melted and annealed at 1550°C, 10 h; OsB_2 (light)+B (dark), etched; ×500

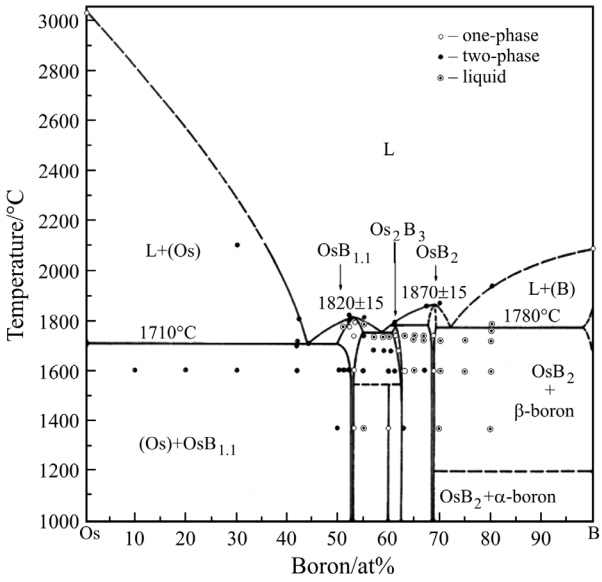

Fig. 7 Os–B phase diagram with $OsB_{1.1}$ (hex.), Os_2B_3 (hex., high and low temperature madification) and OsB_2 phases, respectively

samples at lower temperatures, and since a lot of samples were spent, providing enough information, the transformation in solid was not established.

The $OsB_{1.1}$ phase was determined to melt congruently at 2093±15 K (1820±15°C) and the OsB_2 phase at 2143±20 K (1870±20°C). Solid solubility of boron in osmium was found to be less than 2 at% B.

The phase diagram of Os–B system, according to the obtained results, is presented in Fig. 7. Investigated samples with annealing temperatures, depending on compositions, are shown in a diagram.

Thermodynamic study

Based on the phase diagram of the Os–B binary system, given in Fig. 7, thermodynamic study of the investigated Os–B system was done according to the calculation procedure by Rao and Belton [12].

Alloys in the concentration ranges with x_{Os}=0.5–1 and x_B=0.7–1, respectively, were investigated. For the first interval, osmium-rich side was treated and thermodynamic properties for osmium were determined, and in the second interval, boron-rich side of the phase diagram was investigated and thermodynamic properties for boron were determined.

Values of chosen alloys compositions and adequate liquidus temperatures read from the Os–B phase diagram are shown in Table 1.

In further analysis, thermodynamic properties for the adequate component were calculated considering the calculation procedure given by Eq. (3). The results of this

Table 1 Chosen compositions and adequate liquidus temperatures

xOs	xB	T_{liq}/K
0.05	0.95	2340
0.10	0.90	2317
0.15	0.85	2273
0.20	0.80	2221
0.25	0.75	2132
0.30	0.70	2135
0.50	0.50	2066
0.55	0.45	1999
0.60	0.40	2229
0.65	0.35	2421
0.70	0.30	2577
0.75	0.25	2717
0.80	0.20	2861
0.85	0.15	2969
0.90	0.10	3095
0.95	0.05	3206

calculation include values of $\Delta G^0_{s\to l}$ for boron and osmium at the corresponding liquidus temperature. The activities and activity coefficients for both components in the liquid phase at the liquidus temperature are presented in Table 2.

Table 2 Results of the thermodynamic calculation at the liquidus temperature (energies in J/mol)

xOs	$\Delta G^0_{s\to l}$ (B)	loga_B	a_B	γ_B
0.05	1013	–0.04489	0.902	0.949
0.10	1224	–0.07335	0.845	0.938
0.15	1629	–0.10801	0.779	0.917
0.20	2108	–0.14648	0.714	0.892
0.25	2926	–0.19662	0.636	0.848
0.30	2990	–0.22804	0.592	0.845
xOs	$\Delta G^0_{s\to l}$ (Os)	loga_{Os}	a_{Os}	γ_{Os}
0.50	11494	–0.59159	0.256	0.512
0.55	12063	–0.57480	0.266	0.484
0.60	10073	–0.45787	0.348	0.581
0.65	8341	–0.36702	0.429	0.661
0.70	6898	–0.29470	0.507	0.725
0.75	5583	–0.23226	0.586	0.781
0.80	4311	–0.17561	0.667	0.834
0.85	3183	–0.12657	0.747	0.879
0.90	1973	–0.07905	0.834	0.926
0.95	905	–0.03702	0.918	0.967

The calculation of activities and activity coefficients at investigated temperature of 3500 K, was done according to Eq. (4), assuming regular solution behaviour for the melts, and presented in Table 3. As an illustration, dependencies of osmium and boron activities on composition in temperature interval 3300–3500 K are shown in Fig. 8.

Negative deviation from Raoult's law in the investigated composition ranges could be noticed for both components ($\gamma_{Os}<1$ and $\gamma_B<1$), which means that good miscibility between constitutional components in the osmium–boron system exists. This fact is in the agreement with the phase diagram type, in which numerous osmium borides are formed. Also, it could be noticed that the activity value increase with temperature increasing, becoming closer to the ideal solution line.

Having in mind that, up to now, there are no thermodynamic properties on this system, as well as the fact that extreme high temperatures were taken into the consideration, application of Rao–Belton calculation procedure could be very useful and adequate methodology for thermodynamic investigation of such systems. For further, wider investigation of the Os–B system, thermal analysis techniques should be applied too, having in mind recent research of similar high temperature alloys [13, 14].

Table 3 Calculated thermodynamic properties for osmium and boron

Temp.	3300 K		3400 K		3500 K	
*x*Os	γB	*a*B	γB	*a*B	γB	*a*B
0.05	0.964	0.916	0.965	0.917	0.966	0.918
0.10	0.956	0.861	0.958	0.862	0.959	0.863
0.15	0.942	0.801	0.944	0.802	0.946	0.804
0.20	0.926	0.741	0.928	0.743	0.930	0.744
0.25	0.899	0.674	0.902	0.676	0.904	0.678
0.30	0.897	0.628	0.900	0.630	0.902	0.632
*x*Os	γOs	*a*Os	γOs	*a*Os	γOs	*a*Os
0.50	0.658	0.329	0.666	0.333	0.674	0.337
0.55	0.644	0.354	0.653	0.359	0.661	0.363
0.60	0.693	0.416	0.700	0.420	0.707	0.424
0.65	0.738	0.479	0.745	0.484	0.751	0.488
0.70	0.777	0.544	0.784	0.548	0.789	0.552
0.75	0.816	0.612	0.821	0.616	0.825	0.619
0.80	0.855	0.684	0.859	0.687	0.862	0.689
0.85	0.890	0.757	0.894	0.759	0.896	0.762
0.90	0.931	0.838	0.933	0.839	0.934	0.841
0.95	0.968	0.919	0.968	0.920	0.969	0.921

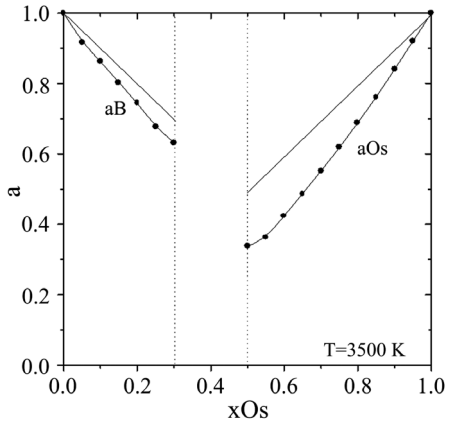

Fig. 8 Dependencies of osmium and boron activities on composition at 3500 K

Conclusions

Phase diagram investigation and thermodynamic study of Os–B system were investigated in this work. The phase diagram was determined by metallographic investiga-

tions and following borides were confirmed: $OsB_{1.1}$ (*hex*.), Os_2B_3 (*hex*.) and OsB_2 (*orthorh.*), while high temperature Os_2B_3 compound with a not yet identified structure was observed. $OsB_{1.1}$ melts congruently at 1820±15°C and OsB_2 at 1870±20°C. The solid solubility of B in Os was found to be less than 0.5 at%B. Thermodynamic study of this system was based on the known liquidus and solidus lines from phase diagram. According to calculation procedure given by Rao and Belton the activities and activity coefficients for osmium and boron were determined in temperature interval 3300–3500 K.

References

1 B. Aronsson, E. Stenberg and J. Aselius, Nature, 195 (1962) 377.
2 B. Aronsson, Acta Chem. Scand., 17 (1963) 2036.
3 T. Lundstram, Coll. Int. du CNRS, 157 (1967) 91.
4 S. Jantsch, L. Politis and L. Stuparević, 5th General Conference of the Condensed Matter Division of the European Physical Society, Berlin 1985, Proceedings, p. 13.
5 E. Hassler, J. Less Comm. Met., 67 (1979) 567.
6 K. Hiebl, J. Less Comm. Met., 82 (1981) 21.
7 P. Rogl, J. Less Comm. Met., 121 (1986) 431.
8 K. Hiebl, J. Less Comm. Met., 117 (1986) 375.
9 P. Rogl, J. Less Comm. Met., 91 (1983) 97.
10 K. Vandenberg *et al*., Mat. Res. Bull., 10 (1975) 889.
11 A. K. Niessen, J. Less Comm. Met., 82 (1981) 75.
12 Y. K. Rao and G. R. Belton, in Chemical Metallurgy – A Tribute to Carl Wagner, Edited by N. A. Gocken, p. 75–96, Metall. Soc. of AIME, Warrendale, Pa., 1981.
13 J. Sunol, A. Gonzales and J. Saurina, J. Therm. Anal. Cal., 72 (2003) 329.
14 H. Saari, D. Y. Seo, J. Blumm and J. Beddoes., J. Therm. Anal. Cal., 73 (2003) 381.